Available online at www.sciencedirect.com
ScienceDirect
International Journal of Heat and Mass Transfer 51 (2008) 1115–1129
International Journal of HEAT and MASS TRANSFER
www.elsevier.com/locate/ijhmt

Wide band cumulative absorption coefficient distribution model for overlapping absorption in H_2O and CO_2 mixtures

Jing He, Way Lee Cheng, Richard O. Buckius *

Department of Mechanical Science and Engineering, University of Illinois at Urbana-Champaign, 1206 West Green Street, Urbana, IL 61801, USA

Received 29 November 2006; received in revised form 5 May 2007
Available online 7 September 2007

Abstract

An accurate wide band cumulative absorption coefficient distribution, $g(k)$, model for thermal radiative transfer in gaseous media containing H_2O and CO_2 is presented. Assuming that the convoluted $g(k)$ function for gas mixture retains the same functional form as the individual gases, the model treats overlapping bands as a "single", complex band with scaled parameters. Corresponding scaling algorithms are proposed for specific overlapping regions. Predictions of the mixture $g(k)$ function and the band absorptance are in good agreement with the line-by-line calculation over a wide range of temperatures from 500 to 2500 K, and pressures up to 10.0 atm. The $g(k)$ model is generally more accurate than the exponential wide band model, and provides comparable accuracy to the statistical narrow-band model in predicting the total emissivity along an isothermal and homogeneous gas column under typical combustion conditions. In addition, this approach significantly enhances the computational efficiency.

Keywords: Radiative transfer; Overlapping; Convolution theorem; Scaling algorithm

1. Introduction

Development of accurate and efficient models for radiative transport in gaseous media is essential in many heat transfer calculations. The cumulative k-distribution, $g(k)$, model has proven to be a powerful method to model radiative heat transfer in non-gray media. The $g(k)$ method formulates radiative properties in terms of the reordered absorption coefficient rather than the spectrally averaged transmissivity or the entire rotational–vibrational band absorptance, thus the method can be directly implemented into radiative transfer equation (RTE) solvers. By sorting the absorption coefficient field into a smooth, monotonously increasing function, the integration over wavenumber is transformed into the integration over the cumulative distribution function which requires only few monochromic quadrature points. The approach significantly reduces the computing time yet retains high accuracy, and can be used in highly non-homogeneous media [1–3], in the presence of scattering particles [2,4], and in arbitrary enclosures.

Most narrow band k-distribution methods employ the analytical cumulative distribution function derived by Lacis and Oinas [2] based upon the Malkmus model, with band parameters obtained from the EM2C database by Soufiani and Taine [5]. Liu et al. [6] indicate that the statistical narrow-band correlated-k model (SNBCK) represents an alternative approach to implement the statistical narrow-band model (SNB). With a commonly used "7-point Gauss–Lobatto" quadrature scheme, the SNBCK model yields comparable accuracy to the original SNB model. Unfortunately, almost all the narrow band k-distribution models share the drawback of having to numerically invert the cumulative distribution function to obtain the absorption coefficient which consumes a significant portion of the total computing time. In order to eliminate this computationally expensive procedure, Liu and Smallwood [7] develop an approach to precalculate the absorption coefficients of real gases and fit the resultant absorption

* Corresponding author. Tel.: +1 217 333 1079; fax: +1 217 244 6534.
E-mail address: buckius@uiuc.edu (R.O. Buckius).

0017-9310/$ - see front matter © 2007 Elsevier Ltd. All rights reserved.
doi:10.1016/j.ijheatmasstransfer.2007.05.014

Nomenclature

A	band absorptance, cm^{-1}
B	pressure broadening parameter (line overlap parameter)
f	distribution function; or blackbody fractional function
g	cumulative absorption coefficient distribution function
k	absorption coefficient, cm^{-1}
P	partial or total pressure, atm
s	ratio between the line intensity and the line spacing, m^2/g
T	temperature, K
u	absorber amount
x	independent variable; or density fraction

Greek symbols

α	integrated band intensity, $cm^{-1}\ m^2/g$
ω	bandwidth parameter, cm^{-1}
ρ	density, g/m^3
τ	optical thickness
η	wavenumber, cm^{-1}
ε	emissivity

Subscripts

0	band center or band head
H_2O, CO_2	water vapor, carbon dioxide
h, c	water vapor, carbon dioxide
i	summation parameter
low	lower limit
up	upper limit

coefficients as a polynomial function of temperature for a chosen quadrature scheme and spectral band structure. However, the applicable range of this approach is limited to low concentrations of radiating gases (typical mole fractions in combustion environment or below) and relatively high temperatures. Other deficiencies, such as the loss in accuracy and sacrifice in flexibility, have also been indicated by the authors.

Denison and Webb [8,9] and Modest et al. [10,11] propose full-spectrum cumulative k-distribution functions (FSK) readily used in engineering calculations for H_2O and CO_2. All are calculated from high resolution spectroscopic databases, such as HITRAN [12], HITEMP [13], and CDSD-1000 for CO_2 [14,15]. Mixture k-distributions can then be obtained from those for individual gases by various algorithms [16] – convolution, superposition, multiplication, and the hybrid approach combing superposition and multiplication, based upon different assumptions on the spectral lines of absorbing species. The formulations of superposition and multiplication are also described by Gerstell [17] in terms of the cumulative optical thickness distribution. Recently, Modest and Riazzi [18] develop a systematic "quasi-convolution" algorithm to assemble full-spectrum k-distributions of a gas mixture from narrow-band k-distributions precalculated for individual species, and accommodate non-gray particle absorption as well as non-gray scattering and non-gray walls. Consequently, a high-accuracy, compact database of narrow-band k-distributions for H_2O and CO_2 has been constructed by Wang and Modest [19], extracted from the latest high resolution spectroscopic databases [13–15]. The accuracy and efficiency of this FSK method rely on a fast access to data files and complex interpolation between precalculated states.

The $g(k)$ method can also be applied in a wide band regime, provided that the scattering properties and the Planck function may be taken to be constants [1]. However, several deficiencies exist in current wide band k-distribution models. The models by Wang and Shi [20], Lee et al. [21], Parthasarathy et al. [22], and Denison and Fiveland [23] have limiting assumptions for overlapping absorption, and the wide band cumulative distribution functions use the band parameters originally developed for the wide band absorptance to estimate the absorption coefficient distribution function. Thus they introduce further approximations and sources of inaccuracy as compared to the associated band model.

The development for a simple yet accurate, fundamentally justified methodology to determine the cumulative k-distribution function based upon the line-by-line calculations is warranted. Marin and Buckius propose a simplified wide band $g(k)$ model for H_2O [24] and CO_2 [25] which explicitly expresses the absorption coefficient in terms of the cumulative distribution function. They also indicate that the appropriate band parameters are dependent on the particular benchmark results used, and a different database would yield a slightly different parameter set [26]. The previous parameters presented in Refs. [24,25] are based upon the HITEMP database [13] for temperatures up to 1000 K, and the EM2C narrow band database [5] above 1000 K. In a very recent study [27], HITEMP is extended to use for temperatures up to 2500 K for H_2O, and the CDSD-1000 database [14,15] is employed for CO_2 which is found more accurate than HITEMP [11,14]. Accurate and computationally efficient polynomial series are evaluated for the three wide band parameters as a function of gas temperature. The improved model shows good agreement in predicting the $g(k)$ function, and provides excellent

results on the band absorptance, for all single bands of H_2O and CO_2 when compared to benchmark calculations.

In the present study, the wide band $g(k)$ model is applied to gas mixtures containing both H_2O and CO_2. The convolution theorem on a narrow or wide band basis is the exact method to predict overlapping properties of a gas mixture. Based upon the analytical behavior of the convolution integral for approximate cumulative distribution functions, the convoluted $g(k)$ function for gas mixture is assumed to retain the same functional form as the individual gases. This assumption provides a model that treats overlapping bands as a "single", complex band with scaled parameters. Wide band scaling equations are developed from basic narrow band models. An enhanced interpolated model is also proposed for the 2.7 μm overlapping band due to the unique characteristic of g-distributions in this particular region. To show the accuracy of the proposed model, root mean errors of the mixture $g(k)$ function, overlapping band absorptance and the total emissivity are presented over a broad range of conditions. The $g(k)$ model is generally more accurate than the exponential wide band model, and achieves comparable accuracy to the statistical narrow-band model in typical combustion environment. In addition, there are significant computational savings. The new parameters developed at ambient pressure [27] can be used accurately in this overlapping model for gas mixtures up to 10.0 atm. Relatively large errors occur in some limiting conditions which are either rare in practical applications or unimportant to combustion problems.

2. Theoretical consideration

2.1. Infrared spectrum

When two or more gases absorb in the same spectral interval, the contribution of band absorption from all radiating species must be included. Fig. 1 illustrates the spectral variation of absorption coefficients for H_2O and CO_2 across the infrared spectrum. Locations of all the important vibrational–rotational bands are also indicated. Note that there are regions in the spectra with significant absorption from both H_2O and CO_2. In this study, the entire spectrum (10–8000 cm^{-1}) is divided into five regions according to the spectral limits of participating H_2O bands specified in Ref. [27].[1] The regions are the rotational overlapping region, the 6.3 μm non-overlapping region, the 2.7 μm overlapping region, the 1.87 μm overlapping region, and the 1.38 μm pure H_2O region. The present model treats the 6.3 μm region as non-overlapping composed by three distinct, separate bands since the overlap between the 6.3 μm H_2O band and the 9.4 μm and 4.3 μm CO_2 bands occurs in H_2O band wings. The boundaries for the defined regions are maintained constant in all conditions. This procedure permits the determination of effective absorption coefficient distribution functions within a specific interval.

2.2. Convolution theorem

The accuracy and computational efficiency of $g(k)$ methods depend on the treatment of overlapping bands. The most commonly accepted approach for overlapping bands is to use the multiplication property of spectrally averaged transmissivity, assuming that the absorption coefficients of participating species are statistically uncorrelated [1,2]. By incorporating the multiplication property directly into the correlated-k method, Goody et al. [1] first derive a convolution integral for the cumulative distribution function of a mixture in terms of distribution functions for the individual gases. However, this approach introduces an optical thickness distribution rather than the absorption coefficient distribution. The paradox is resolved by Zhu [28], who explicitly shows that the convolution theorem for the k-distribution directly results from the multiplication property of band transmission, and the correct convolution formula provides an efficient and accurate method to calculate the composite k-distribution of gas mixtures. The conclusion is further verified by Modest and Riazzi [18]. Through mathematical manipulation on the multiplication equation of spectral transmissivities, they are able to present a single mixture cumulative k-distribution formulation combining individual $g(k)$ functions. They also show that the convolution integration on a narrow-band basis results in small errors compared with direct calculations from the mixture absorption coefficient, and the correlation can be readily extended from a binary mixture to mixtures of arbitrary species.

By comparing the convolution theorem expressed in different forms [18,28,29], a general convolution integral for the mixture $g(k)$ function is written as

$$g(k) = \int_0^{g_2(k)} g_1\left(\frac{k-x}{u_1/u_2}\right) \mathrm{d}g_2(x) = \int_0^{k} g_1\left(\frac{k-x}{u_1/u_2}\right) f_2(x)\,\mathrm{d}x \tag{1}$$

where $g_i(k) = \int_0^k f_i(x)\,\mathrm{d}x$. u_i is defined as the absorber amount [2,28] for species i, given by the optical thickness over the absorption coefficient, τ_i/k_i. u_i can be either geometric pathlength (cm), density pathlength (g/m^2), or pressure pathlength ($atm^{-1}\,cm^{-1}$) depending on the units of the absorption coefficient.

2.3. Convolution integral analysis

There is no general analytical solution to the convolution integral. Therefore it must be evaluated by either approximation or numerical integration. One possible simplification is the so-called 'principal absorber' method proposed by Gerstell [17], assuming that the absorption coefficient is a constant step function for one species of

[1] Comparing with the original divisions in Refs. [24,25], the only change is made to the lower limit of the pure rotational H_2O band, which is extended from 150 cm^{-1} to 10 cm^{-1}.

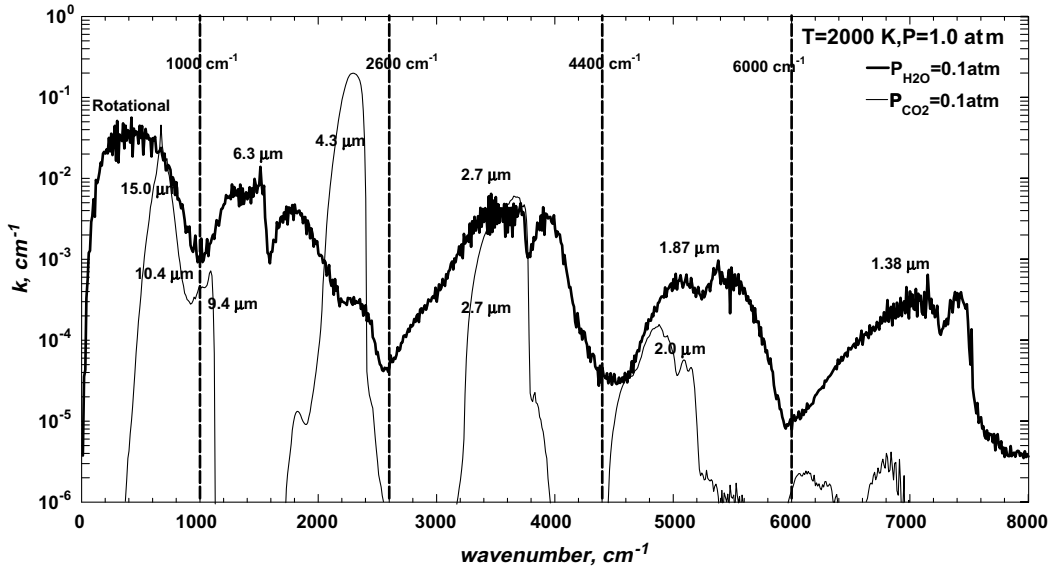

Fig. 1. Absorption coefficient *vs.* wavenumber for H_2O (extracted from HITEMP database [13]) and CO_2 (extracted from CDSD-1000 database [14,15]) at partial pressures of 0.1 atm and $T = 2000$ K across the infrared spectrum, averaged over a spectral interval equal to 10.0 cm^{-1}. The total pressure is 1.0 atm. Locations for all single H_2O and CO_2 bands are indicated in unit of μm. The entire spectrum is divided into five regions, (10, 1000), (1000, 2600), (2600, 4400), (4400, 6000) and (6000, 8000) cm^{-1}, according to the spectral limits of participating H_2O bands specified in Ref. [27].

the mixture. The resulting cumulative distribution function is equal to that of the other gas shifted by this constant in the absorption coefficient. Although this method greatly simplifies the convolution evaluation, it does not represent gas absorption accurately except in liming ranges of mixing ratios.

For overlapping lines of different gases, the volumetric absorption coefficient is generally used, corresponding to the geometric pathlength. In this case, the convolution integral of Eq. (1) reduces to

$$g(k) = \int_0^{g_2(k)} g_1(k-x)\,\mathrm{d}g_2(x) = \int_0^{k} g_1(k-x) f_2(x)\,\mathrm{d}x \qquad (2)$$

In order to analyze the convolution behavior, approximate cumulative distribution functions are substituted into Eq. (2) and then integrated numerically. Fig. 2a and b present the convoluted function resulting from two logarithmic distributions. Individual functions for g_1 and g_2 in Fig. 2a are similar to each other, and the convoluted function, $g(k)$, is no longer logarithmic. However, when g_1 is displaced to much smaller k regions, thus becoming widely separated from g_2 in Fig. 2b, the resulting function coincides with the original function located in the large k regions, $g_2(k)$. This suggests that the convoluted distribution is always dominated by the distribution function with large k values regardless of its functional dependence. The same calculation is performed for two cosinoidal distribution functions, and results are illustrated in Fig. 2c. Unlike the example in Fig. 2a, the resulting function, $g(k)$, now retains the same functional dependence with deferring slopes. And, as the previous example, $g(k)$ is shifted towards larger k regions. Fig. 2d presents a special case in which one of the individual distributions has the Heaviside step function. In this case, the convoluted function is the same as the other distribution with the entire curve shifted towards larger values of k by a constant amount equal to the location of the step.

The fundamental assumption in this wide band $g(k)$ model is that the convoluted distribution function for a gas mixture retains the same functional form as the individual gases. It is concluded from the above examples that this is not accurate for all distributions (Fig. 2a). However, it is valid under some circumstances (Fig. 2c) and in a few limiting cases (Fig. 2d). In some other conditions (Fig. 2b), the assumption is reasonable. Based upon this assumption, the model is able to treat overlapping bands as a "single", complex band with scaled parameters [1,2,31]. Scaling equations for wide band parameters, as well as corresponding algorithms for specific overlapping regions, are presented in the following section.

2.4. Scaling algorithm

2.4.1. Scaling of narrow band parameters

Based upon the Malkmus narrow band model, Lacis and Oinas [2] use the optically thin and optically thick conditions to derive the pressure broadening parameter, B, and the ratio between the line intensity and the line spacing, s, as

$$s = \sum_i x_i s_i \qquad (3)$$

$$\sqrt{Bs} = \sum_i \sqrt{x_i B_i s_i} \qquad (4)$$

x_i is the density fraction for species i,

$$x_i = \frac{\rho_i}{\sum_i \rho_i} \qquad (5)$$

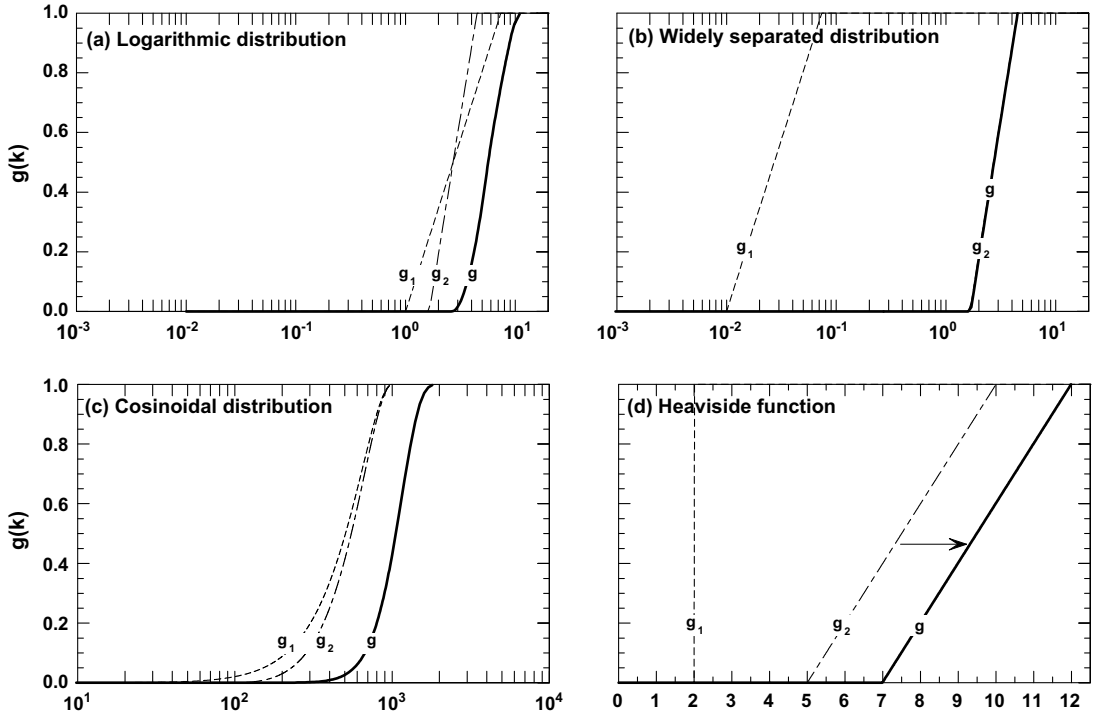

Fig. 2. Convoluted cumulative distribution function, $g(k)$, through numerical integration of Eq. (2) with: (a) two logarithmic functions close to each other:

$$g_1(k)=\begin{cases}0 & k<1\\ \frac{1}{2}\ln(k) & 1\leqslant k\leqslant \mathrm{e}^2\\ 1 & k>\mathrm{e}^2;\end{cases}\quad g_2(k)=\begin{cases}0 & k<\mathrm{e}^{1/2}\\ \ln(k)-\frac{1}{2} & \mathrm{e}^{1/2}\leqslant k\leqslant \mathrm{e}^{3/2}\\ 1 & k>\mathrm{e}^{3/2}\end{cases}$$

(b) two logarithmic functions that are separated widely from each other:

$$g_1(k)=\begin{cases}0 & k<10^{-2}\\ \frac{1}{2}\ln\left(\frac{k}{10^{-2}}\right) & 10^{-2}\leqslant k\leqslant \mathrm{e}^{2+\ln 10^{-2}}\\ 1 & k>\mathrm{e}^{2+\ln 10^{-2}};\end{cases}\quad g_2(k):\ \text{same as (a)}$$

(c) two cosinoidal functions:

$$g_1(k)=\begin{cases}0 & k<10\\ \frac{1}{2}\left[\cos\left(\frac{\pi k}{990}+\frac{98\pi}{99}\right)+1\right] & 10\leqslant k\leqslant 1000\\ 1 & k>1000;\end{cases}\quad g_2(k)=\begin{cases}0 & k<100\\ \frac{1}{2}\left[\cos\left(\frac{\pi k}{900}+\frac{8\pi}{9}\right)+1\right] & 100\leqslant k\leqslant 1000\\ 1 & k>1000\end{cases}$$

(d) one of the individual distributions being the Heaviside step function, and the other being generic.

Alternative scaling methodologies are provided by Liu and coworkers [31], assuming that the product of two Malkmus bands is an approximate Malkmus band.

2.4.2. Scaling of wide band parameters

The exponential wide band model [32] is employed in the present $g(k)$ model, which assumes an exponential profile of the line-intensity-to-spacing ratio in the band wings away from the band center. For a symmetric band, this is expressed as

$$s=\frac{\alpha}{\omega}\exp\left(-\frac{2|\eta-\eta_0|}{\omega}\right) \tag{6}$$

where α is the integrated band intensity, and ω is the bandwidth parameter. Substituting Eq. (6) into Eqs. (3) and (4) leads to

$$\frac{\alpha}{\omega}\exp\left(-\frac{2|\eta-\eta_0|}{\omega}\right)=\sum_i\frac{x_i\alpha_i}{\omega_i}\exp\left(-\frac{2|\eta-\eta_{0,i}|}{\omega_i}\right) \tag{7}$$

$$\sqrt{B\frac{\alpha}{\omega}\exp\left(-\frac{2|\eta-\eta_0|}{\omega}\right)}=\sum_i\sqrt{x_iB_i\frac{\alpha_i}{\omega_i}\exp\left(-\frac{2|\eta-\eta_{0,i}|}{\omega_i}\right)} \tag{8}$$

The summation parameter i denotes all the participating bands in a wide band interval. Integrating Eqs. (7) and (8)

with respect to η across the entire spectrum $(-\infty, +\infty)$ yields two scaling equations for the wide band parameters,

$$\alpha = \sum_i x_i \frac{\alpha_i}{\omega_i} \int_{-\infty}^{+\infty} \exp\left(-\frac{2|\eta-\eta_{0,i}|}{\omega_i}\right) d(\eta-\eta_{0,i}) = \sum_i x_i \alpha_i \tag{9}$$

$$\sqrt{B\alpha\omega} = \sum_i \sqrt{x_i B_i \frac{\alpha_i}{\omega_i}} \int_{-\infty}^{+\infty} \sqrt{\exp\left(-\frac{2|\eta-\eta_{0,i}|}{\omega_i}\right)}\, d(\eta-\eta_{0,i}) = \sum_i \sqrt{x_i B_i \alpha_i \omega_i} \tag{10}$$

The third equation is obtained by noting that the center of the equivalent mixture band, η_0, occurs at the maximum strength of composite lines. For the 2.7 μm, 1.87 μm overlapping regions, the participating bands are approximated as coincident, i.e., $\eta_0 = \eta_{0,1} = \eta_{0,2}$. Evaluation of Eq. (7) at the band center generates the third equation as

$$\frac{\alpha}{\omega} = \sum_i \frac{x_i \alpha_i}{\omega_i} \tag{11}$$

For the rotational overlapping region, the centers of the individual bands are widely separately from each other. If the pure rotational H_2O band center $\eta_{0,1}$, the 15.0 μm CO_2 band center $\eta_{0,2}$, and the 10.4 μm CO_2 band center $\eta_{0,3}$, are substituted into the RHS of Eq. (7), the following three equations are obtained,

$$\begin{aligned} X &= \frac{x_1\alpha_1}{\omega_1} + \frac{x_2\alpha_2}{\omega_2}\exp\left(-\frac{2|\eta_{0,1}-\eta_{0,2}|}{\omega_2}\right) + \frac{x_3\alpha_3}{\omega_3}\exp\left(-\frac{2|\eta_{0,1}-\eta_{0,3}|}{\omega_3}\right) \\ Y &= \frac{x_1\alpha_1}{\omega_1}\exp\left(-\frac{2|\eta_{0,2}-\eta_{0,1}|}{\omega_1}\right) + \frac{x_2\alpha_2}{\omega_2} + \frac{x_3\alpha_3}{\omega_3}\exp\left(-\frac{2|\eta_{0,2}-\eta_{0,3}|}{\omega_3}\right) \\ Z &= \frac{x_1\alpha_1}{\omega_1}\exp\left(-\frac{2|\eta_{0,3}-\eta_{0,1}|}{\omega_1}\right) + \frac{x_2\alpha_2}{\omega_2}\exp\left(-\frac{2|\eta_{0,3}-\eta_{0,2}|}{\omega_2}\right) + \frac{x_3\alpha_3}{\omega_3} \end{aligned} \tag{12a}$$

Assuming that the maximum line-intensity-to-spacing ratio for the equivalent rotational overlapping band is equal to the maximum value among X, Y, Z, the third equation for the rotational region is given by

$$\frac{\alpha}{\omega} = \max(X, Y, Z) \tag{12b}$$

Values for $\eta_{0,1}$, $\eta_{0,2}$, $\eta_{0,3}$ are 140, 667, 960 cm^{-1}, respectively, taken from the latest version of Edwards' exponential wide band model [30].

Denison and Fiveland develop a hybrid wide-band correlated-k weighted-sum-of-gray-gas model [33] for radiative transfer in gas mixtures, where they adopt the same formula developed by Edwards [32] in treating the pure 2.7 μm H_2O band to evaluate the equivalent pressure broadening parameter,

$$\sqrt{B\alpha} = \sum_i \sqrt{x_i B_i \alpha_i} \tag{13}$$

They also propose a modified equation for the bandwidth parameter to account for the separation of the individual bands which applies to the 2.7 μm and the 1.87 μm overlapping regions. After considerable numerical experimentation using the scaled parameters in Ref. [33] and these obtained by (9)–(12), the present scaling equations are found to be more accurate, due to the incorporation of the bandwidth parameter in Eq. (10). While there is only one bandwidth parameter provided by Edwards for the 2.7 μm H_2O band, ω_i varies for different gases in a mixture. Therefore, weighting the parameter B by the products of α and ω, rather than α only, more accurately scales the equivalent overlapping band.

At this stage, the composite cumulative k-distribution function for the three overlapping regions is described by the single $g(k)$ formulation [24,25,27] together with the scaled parameters (Eqs. (9)–(11) or (12)), which will be called the convoluted model in this study. While providing accurate g-distributions for the rotational region and the 1.87 μm region over a wide range of conditions, the convoluted model is found to yield large errors for the 2.7 μm region when CO_2 is dominant in the mixture ($P_{CO_2}/P_{H_2O} \geqslant 2$). Under such circumstances, the assumption that the convoluted $g(k)$ function for mixture retains the same functional form as the individual gases is inaccurate. To increase the accuracy of this overlapping model for general conditions, an alternate model is developed to treat the 2.7 μm overlapping band.

2.5. Enhanced model for the 2.7 μm overlapping band

For the 2.7 μm region, Fig. 1 shows that two broad "transparent" spectral intervals of CO_2 exist in the H_2O band wings where the absorption coefficients of CO_2 are generally orders of magnitudes smaller than H_2O. When such k-variation in wavenumber is transformed into the cumulative k-distribution, the behavior of the mixture $g(k)$ function for small absorption coefficients is dominated by H_2O over a wide range of mixing ratios. Fig. 3 presents the $g(k)$ functions obtained from line-by-line calculations for single radiating gas of H_2O, and for H_2O–CO_2 mixtures at a total pressure of 1.0 atm. A temperature of 2000 K is presented due to the importance of the 2.7 μm region at this temperature. In the limiting case of vanishing H_2O in the mixture (1% by volume as shown in Fig. 3a), the $g(k)$ functions for mixtures corresponding to small absorption coefficients ($g < 0.45$) are very similar to those for only H_2O. This similarity is valid for a wide range of mixing ratios. As H_2O increases, for example 10% in Fig. 3b, the dominance of H_2O is observed regardless of CO_2 concentrations. For even higher concentrations of H_2O as in Fig. 3c, the contribution of CO_2 is further reduced. The mixture $g(k)$ function retains approximately the same functional form as for H_2O. Results predicted by the convoluted model are also presented in Fig. 3. They are accurate for H_2O-rich conditions ($P_{H_2O}/P_{CO_2} > 1$), yet the model significantly over-estimates the absorption coefficient for the small-to-medium g-domain when CO_2 is dominant in the mixture. On the other hand, the convoluted model accurately describes large k regions ($g > 0.8$) in all conditions. Extending the narrow band argument by Lacis and Oinas [2] to wide bands indicates that Eq.

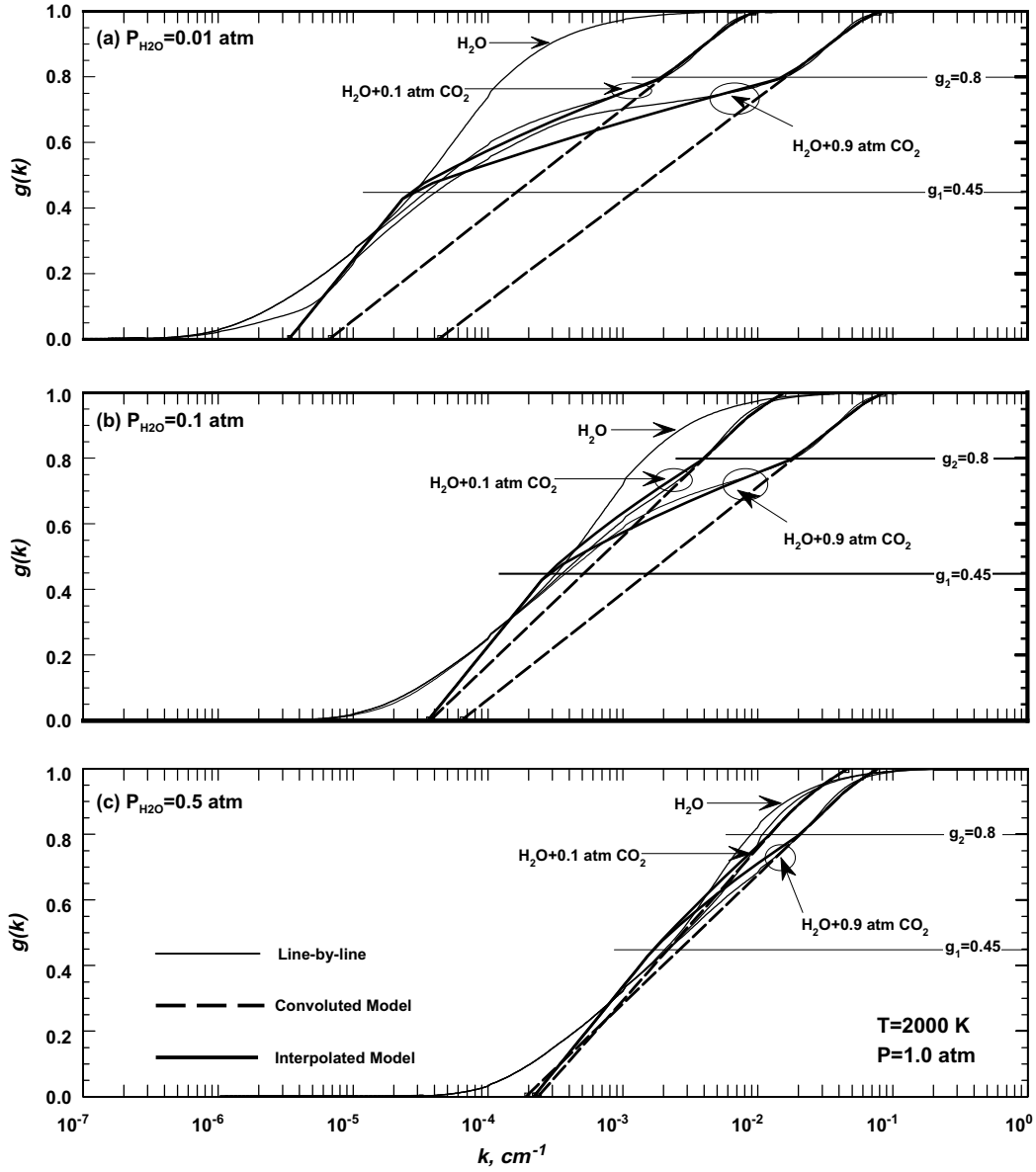

Fig. 3. Cumulative k-distribution function of the 2.7 μm region at 2000 K and 1.0 atm, for single radiating gas of H_2O as well as the indicated H_2O mixing with different CO_2. Partial pressures for H_2O are: (a) $P_{H_2O} = 0.01$ atm, (b) $P_{H_2O} = 0.1$ atm, (c) $P_{H_2O} = 0.5$ atm. The fine solid lines denote the benchmark results by the line-by-line calculation [13–15]; the bold dashed lines represent the convoluted model; the bold solid lines represent the enhanced interpolated model described by Eq. (14).

(10), derived by integration of Eq. (4), implies strong line intensity dependence for both gases. This requirement is satisfied in the band center of the 2.7 μm region, but not in the band wings where H_2O is strongly absorbing and CO_2 is weakly absorbing. Therefore, the combined parameter B is accurate for large absorption, but overestimated by the square root dependence in Eq. (10) for those absorption coefficients corresponding to the small-to-medium g-domain, resulting in the behavior of the convoluted model shown in Fig. 3.

Based upon the above observations, an empirical piecewise function is proposed which divides the g-domain into three subintervals and formulates the absorption coefficient in terms of the cumulative distribution function for each subinterval. The explicit expression of $k(g)$ is developed in Refs. [24,25]. For the small g-domain, $0 \leqslant g \leqslant 0.45$, the absorption coefficient is predicted by the $k(g)$ function for H_2O, denoted as $k_1(g)$, i.e., using band parameters for H_2O as if CO_2 in the mixture is replaced by the same amount of N_2. For the large g-domain, $0.8 \leqslant g \leqslant 1.0$, the convoluted model is employed and it is expressed as $k_2(g)$. A semi-logarithmic interpolation between $k_1(g)$ and $k_2(g)$ (linear on g and logarithmic on k) is used for the absorption coefficient corresponding to the medium g-domain, $0.45 < g < 0.8$. Thus, the proposed piecewise function is given by

Table 1
Summary of the wide band $g(k)$ model

Division of infrared spectrum between 10 and 8000 cm^{-1}	10–1000 cm^{-1}	1000–2600 cm^{-1}	2600–4400 cm^{-1}	4400–6000 cm^{-1}	6000–8000 cm^{-1}
Participating bands					
H_2O	Pure rotational	6.3 μm	2.7 μm	1.87 μm	1.38 μm
CO_2	15.0 μm 10.4 μm	9.4 μm 4.3[a] μm	2.7 μm	2.0 μm	–
Description	Partial overlap (band centers separated)	Non-overlapped (treated as three distinct, separate bands)	Overlapped (band centers coincident)	Overlapped (band centers coincident)	Single H_2O band
$g(k)$ Model[b]	Convoluted model: single $g(k)$ formulation using scaled parameters	Three single $g(k)$	Interpolated model: Eq. (14)	Convoluted model: single $g(k)$ formulation using scaled parameters	Single $g(k)$
Scaling algorithm[c]	$\alpha=\sum_i x_i\alpha_i$	–	$\alpha=\alpha_h$ $\alpha=\sum_i x_i\alpha_i$	$\alpha=\sum_i x_i\alpha_i$	–
	$\omega=\frac{\alpha}{\max(X,Y,Z)}$[d]		k_1: $\omega=\omega_h$ k_2: $\omega=\frac{\alpha}{\frac{x_h a_h}{\omega_h}+\frac{x_c a_c}{\omega_c}}$	$\omega=\frac{\alpha}{\frac{x_h a_h}{\omega_h}+\frac{x_c a_c}{\omega_c}}$	
	$\sqrt{\alpha\omega B}=\sum_i\sqrt{x_i\alpha_i\omega_i B_i}$		$B=B_h$ $\sqrt{\alpha\omega B}=\sum_i\sqrt{x_i\alpha_i\omega_i B_i}$	$\sqrt{\alpha\omega B}=\sum_i\sqrt{x_i\alpha_i\omega_i B_i}$	

[a] Use the multiple band formulation developed in Ref. [27] for the 4.3 μm CO_2 band.
[b] Refer to Refs. [24,25] or [27] for the single $g(k)$ formulation and its analytical inversion $k(g)$.
[c] In the scaling equations, the summation parameter i refers to all the participating bands in a specific overlapping region; the subscript "h", "c" denotes H_2O, CO_2 respectively.
[d] See Eq. (12a) for X, Y, Z.

$$k=\begin{cases} k_1(g), & 0\leqslant g\leqslant 0.45 \\ k_1\exp\left[\left(\frac{g-0.45}{0.8-0.45}\right)\ln\left(\frac{k_2}{k_1}\right)\right], & 0.45<g<0.8 \\ k_2(g), & 0.8\leqslant g\leqslant 1.0 \end{cases} \tag{14}$$

and termed the interpolated model. Performance of this enhanced model is illustrated in Fig. 3. As expected, both models provide accurate results at rich-H_2O conditions, while the interpolated model is more accurate than the convoluted model in the small-to-medium g-domain when the mixture is dominated by CO_2.

Table 1 summarizes the treatments of the present $g(k)$ model, and provides equations for the wide band parameters to be used in corresponding overlapping regions. Note that the three participating bands in the 6.3 μm region are considered as non-overlapping. Total radiative properties for this region are the sum of the contributions from the individual bands. Only a single H_2O band exists in the 1.38 μm region. Thus, there are three combined bands and four single bands to be treated in this wide band $g(k)$ model over the entire spectrum.

3. Model assessment

3.1. Mixture g(k) function and wide band absorptance

The improved wide band parameters for single H_2O and CO_2 bands are developed for one atmospheric pressure and 500–2500 K. The present study indicates that these parameters can be extended to use with high accuracy for gas mixtures up to 10.0 atm. Three pathlength ranges, 0.01–0.1 m, 0.1–10 m, 10–100 m, are used in the analysis of the wide band absorptance. The pathlengths between 0.1 and 10 m are of most concern in practice, being characteristic of industrial combustors and boilers. Note that the 1.38 μm pure H_2O region is excluded in the comparison since the accuracy of the $g(k)$ model for this single H_2O band has been discussed in the previous work [27]. Rather than the 32-point Gaussian quadrature employed in Refs. [24,25,27], a 12-point scheme has been found sufficient for most radiative property calculations.

Table 2a–d present the root mean square errors of the predicted absorption coefficients (RMS_k) and the wide band absorptance (RMS_A) for different spectral regions at the conditions specified in the tables. For combustion applications, 10% H_2O–10% CO_2, 10% H_2O–20% CO_2, and 20% H_2O–10% CO_2 are investigated, which are typical compositions of stoichiometric products of hydrocarbon fuels with different C/H ratios. Two limiting cases, 1% H_2O–90% CO_2 and 90% H_2O–1% CO_2, are also examined to explore the applicability of the $g(k)$ model in extreme conditions. The contribution of temperatures other than the indicated range is small and thus not considered in Table 2.

Table 2a presents the accuracy of the convoluted model for the rotational region. It is observed that the model is in good agreement with the line-by-line calculations, except for gas mixtures containing vanishing H_2O and highly-dominant CO_2 concentrations, where errors as high as 80% are possible. In addition, the RMS_k values are relatively large comparing with the other two overlapping regions (Table 2c and d), above 30% in most conditions. The main reasons for this result are as follows. First, the pure rotational H_2O band model suffers from the

Table 2
Root mean square errors of the predicted absorption coefficients (RMS_k, %) and the wide band absorptance (RMS_A, %), for (a) the rotational region, (b) the 6.3 μm region (RMS_A only; RMS_k inapplicable for this region), (c) the 2.7 μm region, (d) the 1.87 μm region

Pressure		1.0 atm				10.0 atm			
Mole fraction (%)	Temperature (K)	RMS_k (%)	RMS_A (%)			RMS_k (%)	RMS_A (%)		
			0.01–0.1 m	0.1–10 m	10–100 m		0.01–0.1 m	0.1–10 m	10–100 m
(a) Rotational region: (10, 1000) cm^{-1}									
$x_h = 10$; $x_c = 10$	500	33.3	5.3	8.2	3.6	50.7	22.6	11.1	1.7
	1000	32.2	14.8	6.2	4.2	36.4	11.9	3.5	0.9
	1500	52.7	12.9	15.3	5.8	33.5	4.1	5.6	0.7
$x_h = 10$; $x_c = 20$	500	20.8	5.1	2.1	2.7	42.4	17.1	5.8	1.0
	1000	40.3	13.9	10.1	4.3	34.9	6.7	3.7	0.9
	1500	43.9	8.8	12.0	4.3	27.9	4.3	3.7	0.7
$x_h = 20$; $x_c = 10$	500	39.3	3.9	11.4	4.0	53.4	24.2	11.4	1.8
	1000	32.4	10.3	3.1	2.9	39.7	14.7	3.1	1.0
	1500	37.6	12.6	9.3	3.9	31.9	5.7	3.9	0.9
$x_h = 1$; $x_c = 90$	500	76.2	14.6	40.6	56.7	78.5	47.6	60.9	52.3
	1000	65.9	8.5	30.7	41.2	68.9	30.0	45.8	32.5
	1500	55.6	3.7	21.2	27.3	59.2	17.6	32.8	17.0
$x_h = 90$; $x_c = 1$	500	28.0	8.0	6.5	1.5	51.2	16.9	9.9	1.1
	1000	24.7	5.6	4.1	1.4	39.2	9.8	1.5	1.0
	1500	24.3	3.1	3.7	1.0	32.5	5.2	1.3	1.0

Pressure		1.0 atm			10.0 atm		
Mole fraction (%)	Temperature (K)	RMS_A (%)			RMS_A (%)		
		0.01–0.1 m	0.1–10 m	10–100 m	0.01–0.1 m	0.1–10 m	10–100 m
(b) 6.3 μm region: (1000, 2600) cm^{-1}							
$x_h = 10$; $x_c = 10$	500	6.0	1.8	2.8	15.2	16.4	17.4
	1000	1.2	2.8	13.6	6.5	9.7	31.2
	1500	1.2	5.7	23.5	3.3	17.7	34.2
	2000	2.5	6.7	27.1	1.3	20.6	35.5
	2500	2.1	5.8	23.1	1.4	17.4	34.6
$x_h = 10$; $x_c = 20$	500	5.4	3.3	4.7	17.9	18.4	18.5
	1000	1.8	2.4	13.2	7.7	10.5	32.1
	1500	1.8	5.8	23.6	3.2	17.1	34.5
	2000	3.1	6.8	28.1	1.9	20.6	35.5
	2500	2.8	5.1	24.9	1.8	18.3	35.3
$x_h = 20$; $x_c = 10$	500	5.1	1.4	1.6	15.8	13.6	22.4
	1000	1.1	3.3	19.7	6.9	13.7	32.8
	1500	1.5	6.6	29.4	3.3	22.0	34.6
	2000	2.4	7.8	31.6	1.0	23.8	35.4
	2500	2.0	7.0	26.9	1.0	20.2	34.4
$x_h = 1$; $x_c = 90$	500	3.0	15.6	21.9	41.4	36.2	7.3
	1000	1.0	5.2	9.2	18.7	21.9	15.8
	1500	2.1	0.7	2.3	7.1	14.0	22.8
	2000	3.4	1.9	3.8	5.0	9.2	24.7
	2500	2.9	5.6	6.3	7.4	12.0	24.3
$x_h = 90$; $x_c = 1$	500	5.8	3.9	6.5	16.1	8.8	18.8
	1000	3.7	7.0	22.7	8.2	15.3	26.9
	1500	3.8	10.6	25.2	4.4	20.3	29.8
	2000	4.8	11.7	24.5	2.3	20.8	30.8
	2500	5.0	11.2	23.1	1.2	19.6	26.8

Pressure		1.0 atm				10.0 atm			
Mole fraction (%)	Temperature (K)	RMS_k (%)	RMS_A (%)			RMS_k (%)	RMS_A (%)		
			0.01–0.1 m	0.1–10 m	10–100 m		0.01–0.1 m	0.1–10 m	10–100 m
(c) 2.7 μm region: (2600, 4400) cm^{-1}									
(i) Convoluted model									
$x_h = 10$; $x_c = 10$	1000	54.7	9.4	10.2	20.2	63.2	17.2	29.2	31.4
	1500	21.1	11.0	2.5	2.6	32.1	5.1	11.0	7.4
	2000	39.1	5.5	6.8	9.7	16.1	5.2	2.1	1.1
	2500	59.6	2.5	11.8	15.4	30.2	12.8	8.7	2.8

(*continued on next page*)

Table 2 (*continued*)

Pressure		1.0 atm				10.0 atm			
Mole fraction (%)	Temperature (K)	RMS_k (%)	RMS_A (%)			RMS_k (%)	RMS_A (%)		
			0.01–0.1 m	0.1–10 m	10–100 m		0.01–0.1 m	0.1–10 m	10–100 m
$x_h = 10$; $x_c = 20$	1000	64.8	10.8	17.4	29.0	71.5	22.4	37.6	40.9
	1500	24.6	7.8	2.8	6.0	38.3	5.1	14.1	11.9
	2000	54.1	1.3	10.7	12.0	23.1	9.8	5.0	0.9
	2500	95.8	10.2	19.1	20.1	54.5	19.0	14.4	3.2
$x_h = 20$; $x_c = 10$	1000	41.0	6.0	7.0	13.0	51.6	16.4	21.6	17.6
	1000	41.0	6.0	7.0	13.0	51.6	16.4	21.6	17.6
	1500	21.7	10.8	2.2	0.6	26.1	7.3	7.7	2.2
	2000	31.3	9.4	5.1	7.4	18.1	0.5	1.8	0.8
	2500	38.7	3.8	7.8	10.1	21.6	6.8	4.4	1.3
$x_h = 1$; $x_c = 90$	1000	67.8	8.3	13.0	24.9	78.5	20.1	41.4	54.8
	1500	280.3	3.5	24.3	30.1	146.8	10.6	16.9	14.7
	2000	1696	17.9	59.7	82.3	756.8	35.8	61.3	14.1
	2500	3342	29.1	82.1	106.3	1587	49.6	91.5	21.8
$x_h = 90$; $x_c = 1$	1000	16.3	3.2	1.1	3.5	19.9	8.3	1.9	0.1
	1500	21.3	7.5	2.0	3.5	20.8	8.1	2.0	0.1
	2000	23.3	11.1	3.1	2.9	21.8	6.8	2.4	0.1
	2500	23.5	11.1	3.5	2.7	21.8	4.1	2.2	0.1
(ii) Interpolated model [(14)]									
$x_h = 10$; $x_c = 10$	1000	26.6	8.9	7.3	6.0	31.2	13.4	11.8	4.0
	1500	23.2	13.2	5.2	2.4	21.0	4.0	4.8	1.1
	2000	22.8	12.4	5.4	2.5	19.2	0.9	3.1	1.9
	2500	22.2	8.9	4.3	3.2	18.6	3.6	2.7	2.0
$x_h = 10$; $x_c = 20$	1000	32.3	10.1	13.5	9.5	42.4	18.8	17.0	5.6
	1500	21.2	9.9	5.9	2.6	21.2	4.4	5.2	0.3
	2000	18.8	7.4	3.7	2.4	17.3	3.0	2.4	1.6
	2500	17.7	4.4	2.3	3.1	16.6	5.3	2.2	1.9
$x_h = 20$; $x_c = 10$	1000	23.4	5.9	4.4	2.5	23.7	12.3	6.8	1.9
	1500	24.9	13.1	3.8	2.6	21.3	6.2	3.8	0.9
	2000	25.5	14.9	5.3	3.7	21.5	2.7	3.4	1.2
	2500	25.1	12.0	4.9	4.3	21.0	0.9	3.0	1.2
$x_h = 1$; $x_c = 90$	1000	60.3	8.4	13.9	23.5	75.1	20.1	37.4	33.2
	1500	35.6	1.7	2.9	4.2	59.8	1.5	15.8	19.2
	2000	52.3	0.0	5.8	5.2	77.4	4.7	9.4	11.6
	2500	75.1	0.7	6.8	8.0	100.9	3.9	8.5	7.1
$x_h = 90$; $x_c = 1$	1000	16.5	3.3	1.5	3.3	19.5	8.1	1.5	0.1
	1500	21.3	8.2	2.4	3.1	21.0	8.2	2.0	0.1
	2000	23.6	12.1	3.6	2.6	22.0	7.1	2.4	0.1
	2500	24.0	12.2	4.1	2.4	22.0	4.5	2.2	0.1
(d) 1.87 μm region: (4400, 6000) cm^{-1}									
$x_h = 10$; $x_c = 10$	1000	33.6	6.5	7.1	5.6	35.4	13.3	14.0	9.5
	1500	28.0	8.8	5.9	3.2	26.8	7.6	8.4	3.1
	2000	24.9	10.3	6.4	1.5	25.8	0.5	4.8	2.4
	2500	21.8	8.1	5.6	0.6	27.2	5.2	4.0	2.3
$x_h = 10$; $x_c = 20$	1000	34.9	7.6	4.5	8.1	41.6	12.2	16.4	11.3
	1500	29.3	9.7	5.1	4.6	33.7	5.5	10.2	4.4
	2000	26.6	10.8	7.0	3.4	33.4	1.3	6.9	3.1
	2500	23.4	8.1	5.9	3.0	33.9	5.6	5.7	2.7
$x_h = 20$; $x_c = 10$	1000	27.9	6.0	5.2	5.5	30.2	13.3	12.4	7.2
	1500	24.2	8.3	4.7	1.8	23.3	8.4	7.3	1.2
	2000	22.9	9.5	5.2	1.7	23.5	1.6	3.8	1.7
	2500	20.8	7.5	4.5	1.7	26.2	4.6	2.4	1.7
$x_h = 1$; $x_c = 90$	1000	24.0	3.3	1.8	3.5	26.7	5.1	6.6	12.1
	1500	19.5	1.8	1.7	1.5	16.6	7.3	3.3	2.4
	2000	14.0	1.9	2.9	4.6	25.5	8.2	4.6	3.4
	2500	19.1	5.7	6.6	9.0	28.1	0.4	7.0	6.7

Table 2 (*continued*)

Pressure		1.0 atm				10.0 atm			
Mole fraction (%)	Temperature (K)	RMS_k (%)	RMS_A (%)			RMS_k (%)	RMS_A (%)		
			0.01–0.1 m	0.1–10 m	10–100 m		0.01–0.1 m	0.1–10 m	10–100 m
$x_h = 90$; $x_c = 1$	1000	17.0	9.2	4.2	1.4	26.2	13.6	9.5	4.7
	1500	18.5	10.2	4.8	2.3	21.7	8.5	5.8	0.4
	2000	19.0	9.4	5.2	3.0	22.6	2.8	4.1	0.7
	2500	18.3	7.0	4.6	3.1	28.0	3.4	3.0	0.7

For a specified pressure, temperature, and mixture composition, RMS_k is calculated corresponding to $g > 0.2$, and RMS_A is obtained by averaging errors over three pathlength ranges, 0.01–0.1 m, 0.1–10 m, 10–100 m, representative of small, medium and large optical depths, respectively.

inaccurate assumption of a fully symmetric wideband and decaying to zero in both wings since the upper wavenumber portion (140–1000 cm^{-1}) is much wider than the lower wavenumber portion (10–140 cm^{-1}). Second, the combined k-variation for this region cannot be approximated as exponential since the 15.0 μm, 10.4 μm CO_2 bands are located in the pure rotational H_2O band wings to band tails (see Fig. 1). Therefore, use of the spectral form of the exponential wide band model, Eq. (6), does not accurately represent the actual k-variation of gas mixture and introduces error to the predicted $g(k)$ function. On the other hand, the proposed model provides satisfactory results for the band absorptance, with RMS_A typically below 15% except as noted above. The accuracy typically increases for larger optical thickness.

Table 2b presents the accuracy of the predicted band absorptance for the 6.3 μm region, which simply sums the single band absorptance of the 6.3 μm H_2O band, and the 9.4 μm and 4.3 μm CO_2 bands. The multiple band formulation developed in Ref. [27] for the 4.3 μm CO_2 band is

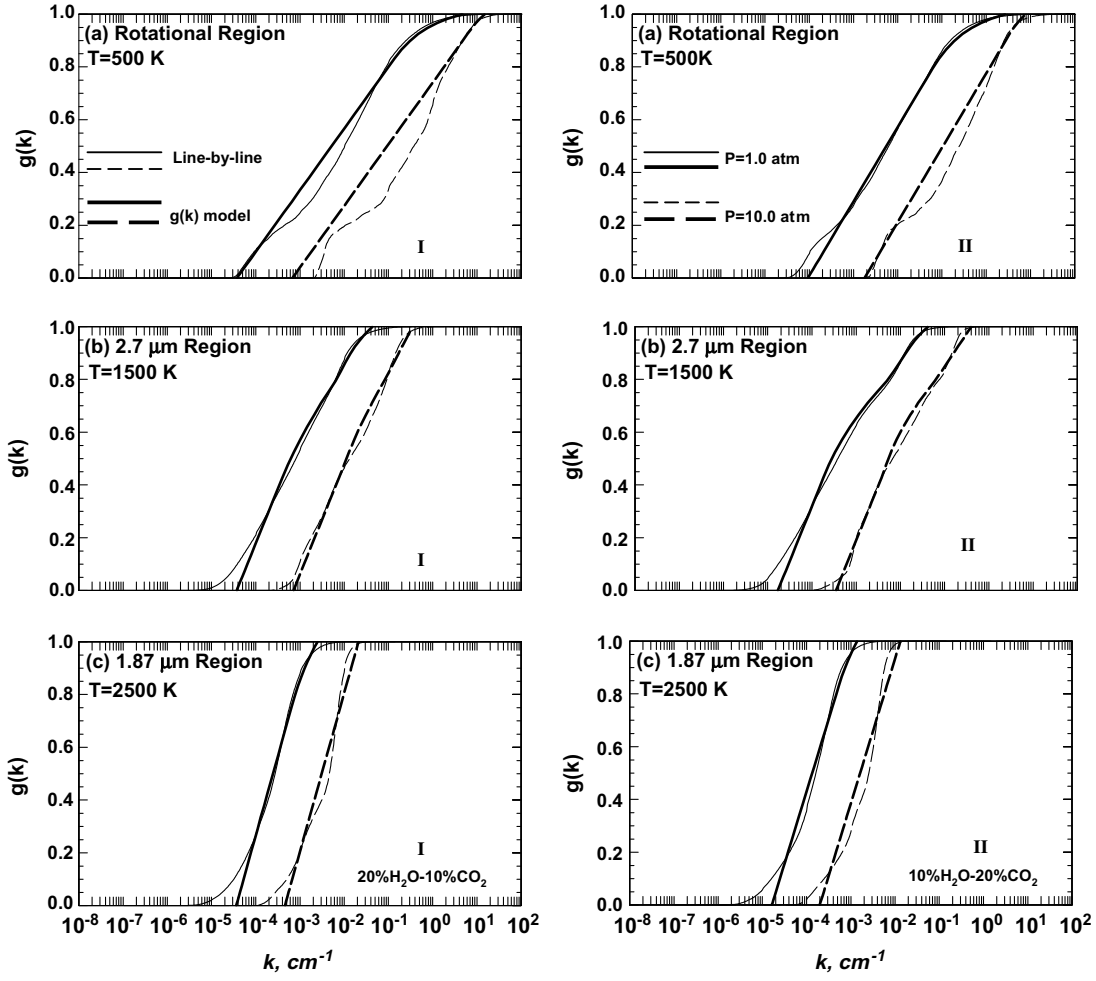

Fig. 4. Cumulative k-distribution function of different overlapping regions for 20% H_2O–10% CO_2 (I) and 10% H_2O–20% CO_2 (II) gas mixtures at total pressures of 1.0, 10.0 atm: (a) the rotational region, (0, 1000) cm^{-1}, at 500 K; (b) the 2.7 μm region, (2600, 4400) cm^{-1}, at 1500 K; (c) the 1.87 μm region, (4400, 6000) cm^{-1}, at 2500 K. The fine lines represent the benchmark results by the line-by-line calculation [13–15]; the bold lines are generated by the wide band $g(k)$ model as described in Table 1.

employed. Table 2b shows good agreement with benchmark calculations. For ambient pressure and small-to-medium pathlengths which are most common in applications, the RMS_A values are generally lower than 10%. The accuracy decreases at higher pressures and larger pathlengths since the "non-overlapping" assumption becomes less accurate as the optical thickness increases. However, the $g(k)$ model can be used within 22% accuracy up to 10.0 atm for small-to-medium pathlengths with a few exceptions at high pressures. Large errors greater than 30% are observed for large pathlengths and high pressures. Under those circumstances, the effect of overlapping, mainly due to the interaction between the 6.3 μm H_2O band and the 4.3 μm CO_2 bands, should be included.

Table 2c presents the accuracy of the prediction on the 2.7 μm region, produced by the convoluted model and the enhanced interpolated model. While the convoluted model is generally less accurate than the interpolated model, results by both models are in reasonable agreement with benchmark calculations for H_2O-rich conditions. As aforementioned, significant errors occur for the convoluted model for gas mixtures dominated by CO_2. In the extreme conditions where the gas mixture is composed by considerable CO_2 and only a small quantity of H_2O, the absorption coefficients are over-estimated significantly. This is explained by the prediction of the convoluted model in the small-to-medium g-domain as illustrated in Fig. 3. Similar errors are observed for the interpolated model. Aside from the specified limiting compositions which are actually rare as combustion products, this enhanced model provides accurate results on the mixture $g(k)$ function and the band absorptance. The RMS_k values typically ranges between 16% and 26%. Larger errors, in the range of 30–40%, occur at 1000 K where the 2.7 μm region is less important. The RMS_A values are below 15% with very few exceptions, and are under 10% for most conditions higher than 1000 K. Due to its accuracy, the interpolated model is employed in the calculation of total radiative properties in the study.

Finally, the usefulness of the convoluted model for the 1.87 μm region is presented in Table 2d, which is accurate throughout the entire domain. The RMS errors of the predicted $g(k)$ function are typically less than 30%. Noticeable errors as high as 42% arise at 1000 K where the 1.87 μm region is less important than the 2.7 μm region. Accordingly, prediction on the band absorptance is excellent, with RMS_A only few percent in most cases and the maximum value less than 17% when compared to the line-by-line results.

Fig. 4 illustrates the cumulative distribution functions of the rotational, 2.7 μm, and 1.87 μm overlapping regions for gas mixtures with typical combustion compositions, obtained from line-by-line calculations and the proposed model described in Table 1. Consistent with the single band model [27], the overlapping model demonstrates good agreement with the benchmark results for large domains of the cumulative distribution function. Differences mainly occur for small values of the absorption coefficient that are of less importance in many engineering applications. Additionally, the small absorption coefficients originate predominately from the band wings which are not accurately modeled, particularly for high temperatures. From Table 2a, the rotational overlapping model generates relatively large errors as compared to the other two regions. It is also noted that the convoluted model loses accuracy in the 1.87 μm region at high pressures since the 2.0 μm CO_2 band is better represented as a multiple band characterized by the presence of distinct and independent rotational–vibrational transitions [26].

3.2. Total emissivity

In the present study, total emissivity calculations are performed for isothermal and homogeneous gas columns to assess the accuracy of the $g(k)$ model. The block approximation [32] is employed, in which the total emissivity is determined by

$$\varepsilon = \sum_{i,\mathrm{Band}} \frac{A_i}{\Delta\eta_i}\left[f\left(\frac{T}{\eta_{\mathrm{low},i}}\right) - f\left(\frac{T}{\eta_{\mathrm{up},i}}\right)\right] \tag{15}$$

where the summation parameter i denotes all the seven bands in the full spectrum, including three combined bands, three individual bands in the 6.3 μm region, and one pure H_2O band in the 1.38 μm region (see Table 1). f is the blackbody fractional function evaluated by the convenient series expansion [34]. Values of the lower limit η_{low}, the upper limit η_{up} and the corresponding spectral interval $\Delta\eta$ (i.e. $\eta_{\mathrm{up}} - \eta_{\mathrm{low}}$) for a particular band, as well as the calculation on the band absorptance A_i, are all provided in Ref. [27].

Table 3 presents the root mean square errors of the predicted total emissivity (RMS_ε) at the indicated conditions. Note that the RMS_ε values are below 10% for a wide range of conditions, comparable to the accuracy of narrow band models. Significant errors occur in two situations. First, for low temperatures (~500 K), small pathlengths (0.01–0.1 m), and low pressures (ambient or few atmospheric pressures), errors between 20% and 40% are observed due to the poor prediction on the rotational region. For this special spectral interval, neither the block approximation nor the band approximation is accurate in computing the emissivity [35]. In addition, notable errors up to 47% occur for the extreme compositions with vanishing H_2O and dominant CO_2 at low temperatures. This is anticipated due to less accuracy of the $g(k)$ model in calculating the band absorptance. However, gas conditions in both situations are less important in practical combustion applications.

Fig. 5 shows the total emissivity of gas mixture containing 20% H_2O–10% CO_2 at 1.0 atm, considered as typical for the combustion of hydrocarbon fuels. Results predicted by the "7-point Gauss–Lobatto" statistical narrow-band correlated-k model (SNBCK-7) [6], the exponential wide

Table 3
Root mean square errors of the total emissivity (RMS_ε, %) for isothermal and homogeneous gas mixtures

Pressure		1.0 atm			10.0 atm		
Mole fraction (%)	Temperature (K)	RMS_ε (%)			RMS_ε (%)		
		0.01–0.1 m	0.1–10 m	10–100 m	0.01–0.1 m	0.1–10 m	10–100 m
$x_h = 10$; $x_c = 10$	500	27.8	8.6	1.0	8.9	10.8	6.7
	1000	7.1	6.8	8.4	2.2	4.4	13.2
	1500	1.5	6.0	9.5	1.1	5.9	8.6
	2000	1.4	3.0	7.4	1.5	4.4	3.3
	2500	1.6	2.3	5.1	2.8	3.6	2.4
$x_h = 10$; $x_c = 20$	500	21.6	8.4	0.4	8.1	10.2	7.1
	1000	5.3	4.8	6.6	3.8	4.8	12.8
	1500	1.5	4.2	8.2	0.3	4.3	7.8
	2000	1.3	2.5	6.4	1.2	3.5	2.6
	2500	1.4	2.0	4.3	2.4	3.2	2.4
$x_h = 20$; $x_c = 10$	500	27.7	6.4	0.9	11.4	10.2	9.4
	1000	9.6	7.0	12.1	2.7	6.8	14.7
	1500	2.9	6.7	11.1	0.8	7.4	8.2
	2000	1.1	3.9	7.4	1.6	4.6	2.3
	2500	1.3	2.8	4.3	3.4	3.0	4.6
$x_h = 1$; $x_c = 90$	500	14.1	28.5	37.8	42.5	47.4	27.5
	1000	5.2	12.6	17.4	21.1	29.3	12.1
	1500	3.0	4.4	6.2	7.2	14.6	7.4
	2000	4.2	4.2	3.2	3.5	7.6	6.4
	2500	3.6	3.8	1.9	2.7	4.6	6.4
$x_h = 90$; $x_c = 1$	500	20.9	3.8	0.5	10.1	10.8	8.2
	1000	10.6	7.6	14.3	2.5	8.5	12.2
	1500	5.1	6.0	8.7	1.2	6.8	5.3
	2000	0.9	2.9	2.8	0.3	2.9	3.1
	2500	1.2	1.1	2.5	2.4	2.6	10.2

For a specified pressure, temperature, and composition, the errors produced by the $g(k)$ model are averaged over three ranges of pathlengths, 0.01–0.1 m, 0.1–10 m, 10–100 m, representative of small, medium and large optical depth, respectively.

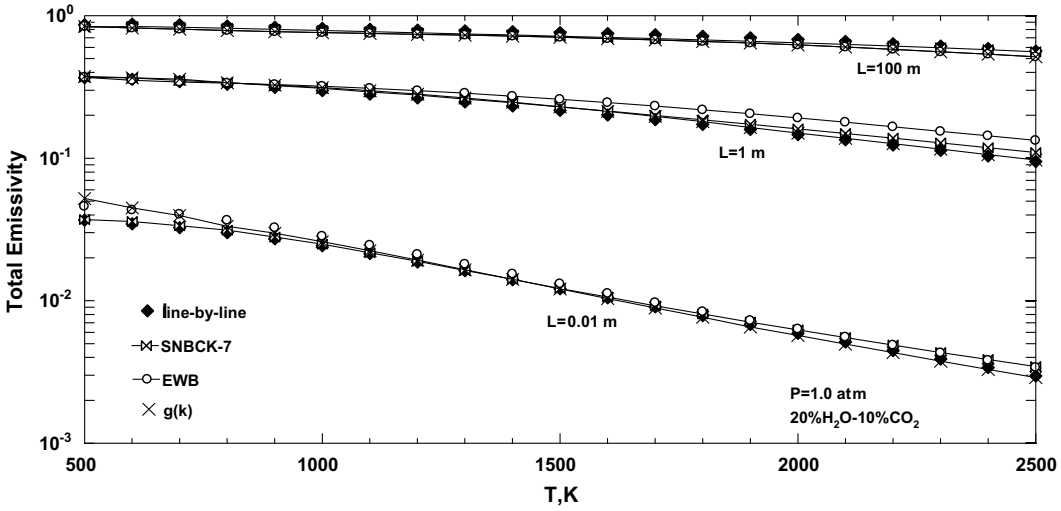

Fig. 5. Total emissivity of 20% H_2O–10% CO_2 isothermal and homogeneous gas mixture at 1.0 atm, for varying temperatures and pathlengths. Results predicted by the "7-point Gauss–Lobatto" statistical narrow-band correlated-k model (SNBCK-7) [6], the exponential wide band model (EWB) [32], and the present wide band $g(k)$ model as described in Table 1 are presented and compared with the line-by-line calculation [13–15].

band model (EWB) [32], and the wide band $g(k)$ model are presented and compared with the line-by-line calculations [13–15]. The $g(k)$ model is observed to be in excellent agreement with the line-by-line calculation except at low temperatures (<800 K) and small pathlengths. Otherwise, the model is comparable to the statistical narrow-band model, and outperforms the associated exponential wide band model for most cases.

3.3. Computational efficiency

The computational efficiency of $g(k)$ methods is determined by three factors: (i) evaluation of the absorption coefficient from the cumulative distribution function; (ii) quadrature scheme; and (iii) number of spectral intervals. The absorption coefficients in the SNBCK model are generally obtained iteratively, using, for example, the Newton–Raphson method. Such a numerical inversion of the cumulative distribution function consumes a significant portion of the total computing time [7]. Since the current $g(k)$ model is analytically invertable, it provides an explicit expression for the absorption coefficient in terms of the cumulative distribution function. The only exception is the multiple band formulation for the 4.3 μm CO_2 band which requires numerical inversion. Along a single line-of-sight, the number of RTE evaluations for the entire spectrum is equal to the product of the number of quadrature points and the number of spectral bands. There are 367 narrow bands for H_2O, and 96 narrow bands for CO_2 which are all overlapping with H_2O bands in the EM2C database [5]. Therefore, if the SNBCK-7 model is employed, the RTE has to be evaluated 2569 times for H_2O and 672 times for CO_2. In case of H_2O–CO_2 mixtures, the computing time increases quadratically with the quadrature points for overlapping bands if the spectra of the two absorbing gases are assumed to be completely uncorrelated. This makes the SNBCK model very slow in handling overlapping absorption. On the other hand, the wide band $g(k)$ model involves only five important rotational–vibrational bands for H_2O, and six for CO_2. By treating the overlapping band as a "single", complex band, the model introduces little additional computational burden as compared to one absorbing gas. Hence, using the proposed $g(k)$ model together with a 12-point Gaussian quadrature scheme, the number of evaluations is reduced by a factor of approximately 10^2 for a mixture.

4. Conclusions

An accurate and computationally efficient wide band $g(k)$ model is presented in this study on overlapping absorption in H_2O–CO_2 gas mixtures, for use in the temperature range 500–2500 K, and total pressures from 1.0 atm up to 10.0 atm. The entire infrared spectrum is divided into five spectral regions and maintained constant in all conditions, including three overlapping regions, one non-overlapping region and one pure H_2O region. Assuming that the convoluted $g(k)$ function for gas mixture retains the same functional form as the individual gases, the model treats overlapping bands as a "single", complex band with scaled wide band parameters. An empirical interpolated formulation is proposed to improve the prediction for the 2.7 μm region based upon the observation of real g-distributions. The accuracy of the predicted $g(k)$ function, band absorptance, and the total emissivity is provided for isothermal and homogeneous gas columns in typical combustion environments, as well as other limiting situations. The results show that the $g(k)$ model is generally more accurate than the exponential wide band model and yields comparable accuracy to narrow band models in typical combustion conditions. Relatively large errors between 20% and 40% occur at low temperatures around 500 K and small pathlengths in the range 0.01–0.1 m. Note that this error is of the same order as the original exponential wide band model. Large errors up to 50% arise for the limiting conditions where the temperature is relatively low (<1000 K) and the gas mixture is dominated by CO_2. Extensive calculations indicate that the model can be used for mole fractions of H_2O greater than a few percent in the mixture. Compared to the SNBCK model, the $g(k)$ model significantly reduces the computational requirements.

References

[1] R. Goody, R. West, L. Chen, D. Crisp, The correlated-k method for radiation calculations in nonhomogeneous atmospheres, J. Quant. Spectrosc. Radiat. Transfer 42 (6) (1989) 539–550.
[2] A.A. Lacis, V. Oinas, A description of the correlated k distribution method for modeling nongray gaseous absorption, thermal emission, and multiple scattering in vertically inhomogeneous atmospheres, J. Geophys. Res. 96 (D5) (1991) 9027–9063.
[3] O. Marin, R.O. Buckius, Wide band correlated-k approach to thermal radiative transport in nonhomogeneous media, J. Heat Transfer 119 (1997) 719–729.
[4] O. Marin, R.O. Buckius, Wideband correlated-k method applied to absorbing, emitting, and scattering media, J. Thermophys. Heat Transfer 10 (2) (1996) 364–371.
[5] A. Soufiani, J. Taine, High temperature gas radiative property parameters of statistical narrow-band model for H_2O, CO_2 and CO, and correlated-k model for H_2O and CO_2, Int. J. Heat Mass Transfer 40 (4) (1997) 987–991.
[6] F. Liu, G.J. Smallwood, Ö.L. Gülder, Application of the statistical narrow-band correlated-k method to low-resolution spectral intensity and radiative heat transfer calculations – effects of the quadrature scheme, Int. J. Heat Mass Transfer 43 (2000) 3119–3135.
[7] F. Liu, G.J. Smallwood, An efficient approach for the implementation of the SNB based correlated-k method and its evaluation, J. Quant. Spectrosc. Radiat. Transfer 84 (2004) 465–475.
[8] M.K. Denison, B.W. Webb, An absorption-line blackbody distribution function for efficient calculation of total gas radiative transfer, J. Quant. Spectrosc. Radiat. Transfer 50 (5) (1993) 499–510.
[9] M.K. Denison, B.W. Webb, Development and application of an absorption-line blackbody distribution function for CO_2, Int. J. Heat Mass Transfer 38 (10) (1995) 1813–1821.
[10] M.F. Modest, V. Singh, Engineering correlations for full spectrum k-distributions of H_2O from the HITEMP spectroscopic databank, J. Quant. Spectrosc. Radiat. Transfer 93 (2005) 263–271.
[11] M.F. Modest, R.S. Mehta, Full spectrum k-distribution correlations for CO_2 from the CDSD-1000 spectroscopic databank, Int. J. Heat Mass Transfer 47 (2004) 2487–2491.
[12] L.S. Rothman, R.R. Gamache, R.H. Tipping, C.P. Rinsland, M.A.H. Smith, D.C. Benner, V.M. Devi, J.-M. Flaud, C. Camy-Peyret, A. Perrin, A. Goldman, S.T. Massie, L.R. Brown, R.A. Toth, The HITRAN molecular database: editions of 1991 and 1992, J. Quant. Spectrosc. Radiat. Transfer 48 (5–6) (1992) 469–507.
[13] L.S. Rothman, C. Camy-Peyret, J.-M. Flaud, R.R. Gamache, A. Goldman, D. Goorvitch, R.L. Hawkins, J. Schroeder, J.E.A. Selby,

R.B. Wattson, HITEMP, the high-temperature molecular spectroscopic database 2000, Available from: <http://www.hitran.com>.
[14] S.A. Tashkun, V.I. Perevalov, J.-L. Teffo, A.D. Bykov, N.N. Lavrentieva, CDSD-1000, the high-temperature carbon dioxide spectroscopic databank, J. Quant. Spectrosc. Radiat. Transfer 82 (1–4) (2003) 165–196.
[15] S.A. Tashkun, V.I. Perevalov, A.D. Bykov, N.N. Lavrentieva, J.-L. Teffo, Carbon dioxide spectroscopic databank (CDSD) 2000, Available from: <ftp://ftp.iao.ru/pub/CDSD-1000>.
[16] V.P. Solovjov, B.W. Webb, SLW modeling of radiative transfer in multicomponent gas mixtures, J. Quant. Spectrosc. Radiat. Transfer 65 (2000) 655–672.
[17] M.F. Gerstell, Obtaining the cumulative *k*-distribution of a gas mixture from those of its components, J. Quant. Spectrosc. Radiat. Transfer 49 (1) (1993) 15–38.
[18] M.F. Modest, R.J. Riazzi, Assembly of full-spectrum *k*-distributions from a narrow-band database; effects of mixing gases, gases and nongray absorbing particles, and mixing with nongray scatters in nongray enclosures, J. Quant. Spectrosc. Radiat. Transfer 90 (2005) 169–189.
[19] A. Wang, M.F. Modest, High-accuracy, compact database of narrow-band *k*-distributions for water vapor and carbon dioxide, J. Quant. Spectrosc. Radiat. Transfer 93 (2005) 245–261.
[20] W.C. Wang, G.Y. Shi, Total band absorptance and *k*-distribution function for atmospheric gases, J. Quant. Spectrosc. Radiat. Transfer 39 (5) (1988) 387–397.
[21] P.Y.C. Lee, K.G.T. Hollands, G.D. Raithby, Reordering the absorption coefficient within the wide band for predicting gaseous radiant exchange, ASME J. Heat Transfer 118 (1996) 394–400.
[22] G. Parthasarathy, J.C. Chai, S.V. Patankar, A simple approach to non-gray gas modeling, Numer. Heat Transfer Part B 29 (1996) 113–123.
[23] M.K. Denison, W.A. Fiveland, A correlation for the reordered wave number of the wide-band absorptance of radiating gases, ASME J. Heat Transfer 119 (1997) 853–856.
[24] O. Marin, R.O. Buckius, A simplified wide band model of the cumulative distribution function for water vapor, Int. J. Heat Mass Transfer 41 (1998) 2877–2892.
[25] O. Marin, R.O. Buckius, A simplified wide band model of the cumulative distribution function for carbon dioxide, Int. J. Heat Mass Transfer 41 (1998) 3881–3897.
[26] O. Marin, R.O. Buckius, A model of the cumulative distribution function for wide band radiative properties, J. Quant. Spectrosc. Radiat. Transfer 59 (1998) 671–685.
[27] J. He, R.O. Buckius, Improved band parameters for a simplified wide band cumulative absorption coefficient distribution model for H_2O and CO_2, Int. J. Heat Mass Transfer, doi:10.1016/j.ijheatmasstransfer.2007.07.016 (submitted for publication).
[28] X. Zhu, On overlapping absorption of a gas mixture, Theor. Appl. Climatol. 52 (1995) 135–142.
[29] M.K. Denison, B.W. Webb, The spectral-line weighted-sum-of-gray-gases model for H_2O/CO_2 mixtures, ASME J. Heat Transfer 117 (1995) 788–792.
[30] M.F. Modest, Radiative Heat Transfer, second ed., Academic Press, 2003.
[31] F. Liu, G.J. Smallwood, Ö.L. Gülder, Application of the statistical narrow-band correlated-*k* method to non-grey gas radiation in CO_2-H_2O mixtures: approximate treatments of overlapping bands, J. Quant. Spectrosc. Radiat. Transfer 68 (2001) 401–417.
[32] D.K. Edwards, Molecular gas band radiation, Advances in Heat Transfer, vol. 12, Academic Press, New York, 1976.
[33] M.K. Denison, W.A. Fiveland, A hybrid wide-band correlated-*k* weighted-sum-of-gray-gas model for radiative transfer in non-homogeneous gas mixtures, HTD-Vol. 345, in: ASME Proceedings of the 32nd National Heat Transfer Conference, vol. 7, 1997, pp. 13–22.
[34] R. Siegel, J.R. Howell, Thermal Radiation Heat Transfer, fourth ed., Taylor & Francis, New York, 2002.
[35] T.T. Charalampopoulos, J.D. Felske, Total band absorptance, emissivity, and absorptivity of the pure rotational band of water vapor, J. Quant. Spectrosc. Radiat. Transfer 30 (1983) 89–96.